

Excellence in Chemistry Research

Announcing our new flagship journal

- Gold Open Access
- Publishing charges waived
- Preprints welcome
- Edited by active scientists



Meet the Editors of *ChemistryEurope*



Luisa De Cola

Università degli Studi
di Milano Statale, Italy



Ive Hermans

University of
Wisconsin-Madison, USA

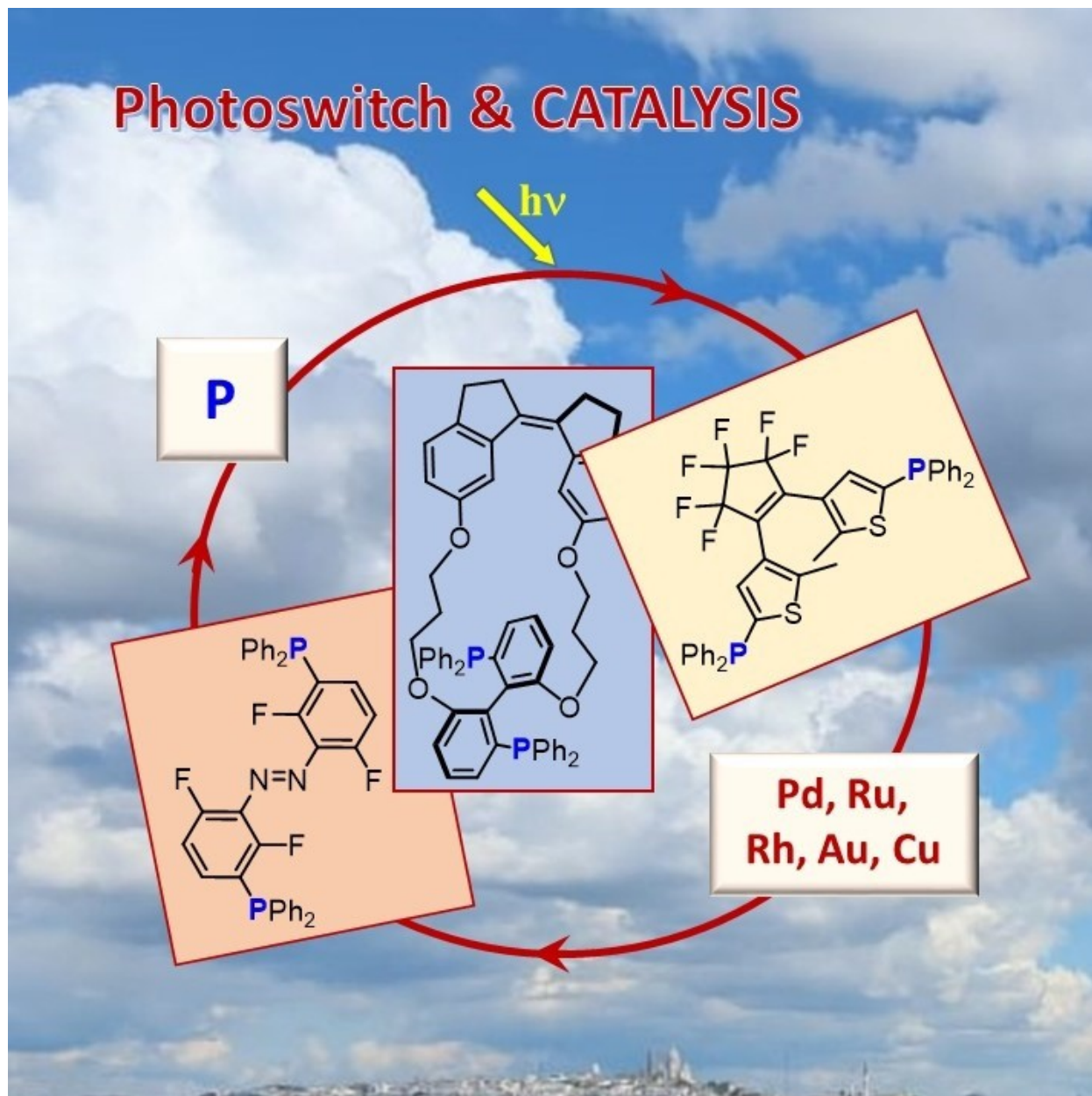


Ken Tanaka

Tokyo Institute of
Technology, Japan

Photoswitchable phosphines in catalysis

Fabrizio Medici,^[a] Nawel Goual,^[a] Vincent Delattre,^[a] Arnaud Voituriez,^{*[a]} and Angela Marinetti^{*[a]}



Photoswitchable catalysts based on phosphorus ligands have been overlooked so far, despite the growing current interest for catalysts control through external stimuli. This review surveys the current knowledge in the field, including synthetic approaches to photoswitchable phosphines and their transition metal complexes, and applications in rhodium, palladium, gold,

ruthenium and copper catalysis. This survey demonstrates that both regulation of the catalytic activity and tuning of the chemo- and enantioselectivity can be achieved using irradiation as a non-invasive external stimulus. Non-catalytic uses of photoswitchable phosphines in organic synthesis are also mentioned.

1. Introduction

Molecular photoswitches have received attention as suitable tools for the non-invasive, external control and modulation of biological systems,^[1] as well as for the miniaturization of key technologies: nanoscale electronic devices,^[2] artificial molecular machines,^[3] functional materials^[4] and energy storage devices,^[5] among others. Moreover, photoswitch phenomena have been considered in the field of homogeneous catalysis, with the aim to mimic the dynamic behaviour of bio-catalysts that regulate their catalytic activity via subtle conformational changes.^[6] Notably, photoresponsive oxazoline-Cu complexes,^[7] NHC ligands^[8] and a number of organocatalysts^[9] have been investigated, by targeting product control, ON/OFF switch of the catalytic activity and enantioselectivity tuning. However, studies on photoswitchable phosphines and their catalytic uses have been rarely disclosed so far, despite the key role of phosphines in both organometallic and organocatalysis.

This short review intends to survey the current knowledge in this overlooked field, so as to hopefully stimulate more extended future developments. This paper will summarize the main synthetic approaches to photoresponsive phosphines and their metal complexes, as well as the known examples of catalytic switches. A non-catalytic use of photoswitchable phosphines in organic synthesis is also illustrated.

2. Synthesis of photoswitchable phosphines

Synthetic strategies toward photoresponsive phosphines rest on three well-known photochromic moieties, namely azobenzenes, dithienylethenes and 1,1'-biindanes (Scheme 1), to which phosphorus functions can be appended easily.

Azobenzenes are known to toggle between E- and metastable Z-forms under irradiation with UV light, while the reverse process takes place either thermally (T-type chromophores) or under irradiation with visible light.^[10] Dithienylethenes, typified in Scheme 1 by dithienylcyclopentenes, are P-type chromophores undergoing conrotatory ring-closure/

ring opening reactions under irradiation at different wavelengths.^[11] Finally, 1,1'-biindanes belong to the family of overcrowded alkenes^[12] that alternate between E and Z isomeric forms when irradiated in the UV and visible range respectively (P-type chromophores).

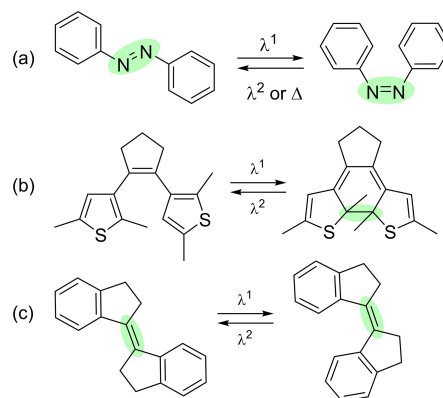
The synthetic approaches to phosphines based on these three photoswitchable backbones are typified hereafter.

2.1. Azobenzene derived phosphines

Phosphines displaying azobenzene units are easily available by either forming the azo linkage from suitably functionalized aryl-phosphines or by late introduction of phosphorus on preformed azobenzenes.

In the late nineties, K. R. Flower first demonstrated that the aromatic electrophilic substitutions of arenediazonium tetrafluoroborates on naphthols or phenols tolerate trivalent phosphine and phosphine sulfide functions, allowing the synthesis of the azobenzene-phosphine derivatives 1–3 in Scheme 2.^[13] The regioselectivity of these reactions is controlled by the *ortho/para*-directing effects of the OH functions of the substrates. Phosphines 1 a–g formally display an azo linkage, but exist primarily as the hydrazone tautomers 1'. Tautomerization can be prevented by O-acylation that leads thus to defined azobenzene moieties (1 h).

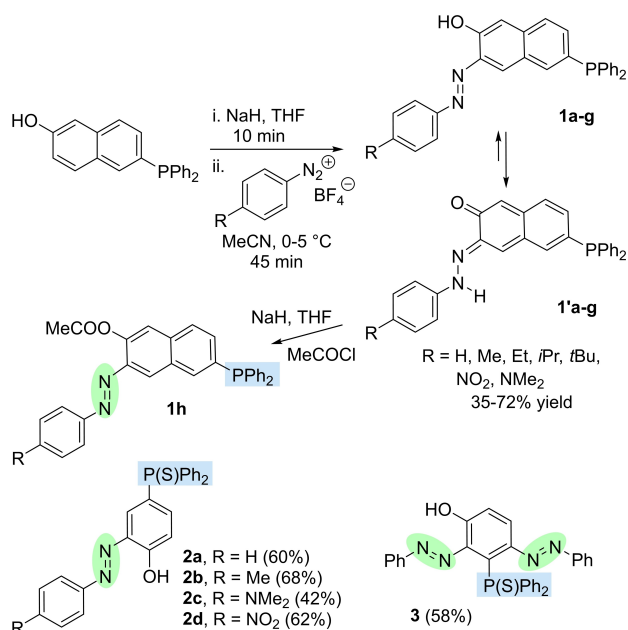
Alternatively, the azo-linkage can be created through dehydrative condensation of aminoaryl-phosphines with appropriate nitrosobenzenes (Mills reaction). As illustrated in Scheme 3, the method has been applied to the synthesis of the first axially chiral azobenzene-phosphine (S)-4 that displays a binaphthyl core.^[14]



Scheme 1. Structural units for the engineering of photoresponsive trivalent phosphines: (a) azobenzenes, (b) dithienylethenes, (c) biindanes.

[a] Dr. F. Medici, N. Goual, V. Delattre, Dr. A. Voituriez, Dr. A. Marinetti
Université Paris-Saclay
CNRS, Institut de Chimie des Substances Naturelles, UPR 2301
91198, Gif-sur-Yvette (France)
E-mail: arnaud.voituriez@cnsr.fr
angela.marinetti@cnsr.fr

P This publication is part of a Special Collection on "Phosphorus in Catalysis". Please check the ChemCatChem homepage for more articles in the collection.



Scheme 2. Synthesis of azobenzene-phosphines and phosphine sulfides from arenediazonium salts by electrophilic aromatic substitutions on naphthols or phenols.



Scheme 3. Condensation of an amino-phosphine with nitrosoaryls.

Beyond the few examples above, the most general synthetic method remains the introduction of phosphorus functions on preformed iodo- or bromo-azobenzenes, *via* either a halogen-lithium exchange/phosphination sequence, or by palladium-promoted couplings with secondary phosphines. The lithiation-phosphination method has been used initially for the synthesis of the amino-substituted mono-phosphine **5 a** (Scheme 4a), with the purpose to investigate the nonlinear optical properties of the corresponding oxides, e.g. **5 b**, and phosphonium salts.^[15] Later, the parent mono-phosphine, *p*-Ph₂P–C₆H₄–N=N–C₆H₅ **6 a**,^[16] and the mono- and diphosphines **7** and **8**, with fluoro-substituted azobenzene units, have been obtained in good yields by the same method (Scheme 4b). In the last two examples, the lithiation step must be carried out at very low temperature (–95 °C to –130 °C) to reach good yields.^[17] Also, phosphines **9 a–c** that



Vincent Delattre studied chemistry at the National Graduate School of Chemistry of Montpellier (ENSCM) where he obtained his Master Degree in 2018. After two internships in pharmaceutical companies, he started his PhD at the ICSN, under the supervision of Dr A. Marinetti, working on photoswitchable bifunctional phosphines and applications in catalysis.



Nawel Goual was awarded with a M. Sc. degree in 2018 from the Université Paris-Est Créteil (UPEC). She got trainings at the Institut de Chimie et Matériaux Paris Est in 2016–17 and at the ICSN in 2018. In October 2018, she joined the ‘Phosphorus Chemistry and Catalysis’ group at the ICSN as a PhD student, under the supervision of Dr. A. Voituriez. Her PhD work focuses on the development of new photoswitchable backbones and the synthesis and catalytic applications of photoresponsive diphosphines.



Angela Marinetti is a CNRS Research Director. She started her career in 1981 as a member of the research group headed by Dr François Mathey (CNRS, Ecole Polytechnique). In 1997 she moved to the ChimieParisTech Engineering School (former ENSCP) and in 2005 she joined the ICSN as a team leader. From 2015 to 2019 she has been Director of this Institute. Her current scientific interests are mainly related to the design, synthesis and catalytic

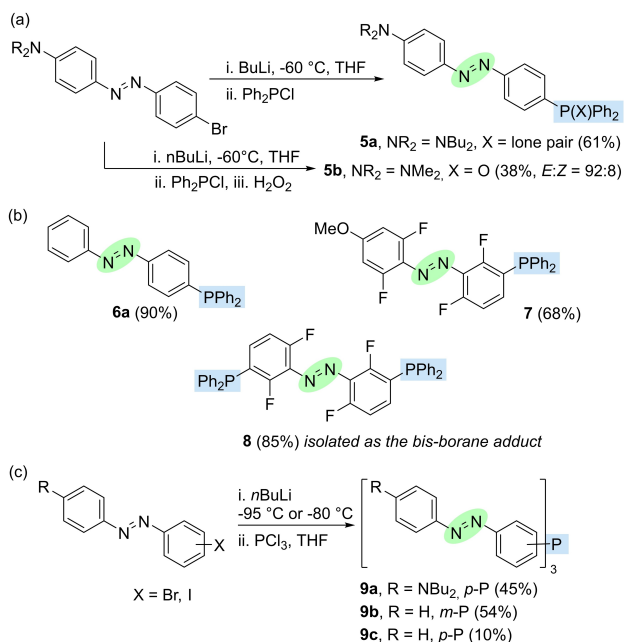


applications of chiral phosphorus ligands and organocatalysts.

Fabrizio Medici was awarded with a M. Sc. degree in 2014 from the University of Insubria (Italy). He obtained a PhD in Molecular Chemistry in 2017 at Sorbonne Université (Paris), under the supervision of Prof. L. Fensterbank and Dr. G. Lemiere. In 2018 he joined the ICSN as a post-doctoral fellow, working on photoswitchable diphosphine gold(I) complexes under the supervision of Dr. A. Marinetti and Dr. A. Voituriez. Since 2019, he holds a post-doctoral position at the University of Milan, working with Prof. M. Benaglia and Pr. A. Puglisi.



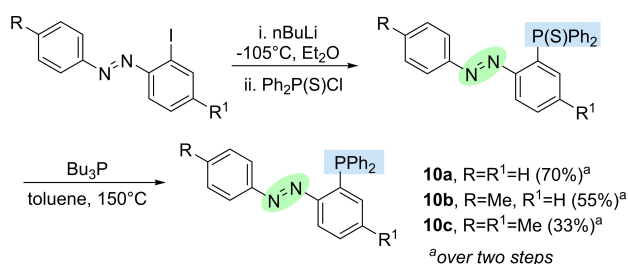
Arnaud Voituriez received his Ph.D. from the University of Paris-Sud (Orsay) in 2004, under the supervision of Dr. E. Schulz. After post-doctoral trainings in the groups of Prof A.B. Charette (Montreal, Canada) and Prof F. Chemla (Paris VI, France) he was appointed at the CNRS in 2007, at the ICSN. In 2012 he received his HDR diploma (Habilitation to conduct research) and became a CNRS Research Director in 2016. His current research interests include: 1) Synthesis of new chiral phosphines and applications in asymmetric organocatalysis; 2) Synthesis of new phosphahelicenes; 3) Enantioselective gold(I)-catalysis and applications in synthesis; 4) Development of new (asymmetric) reactions *via* P^(V)/P^(III) redox cycling.



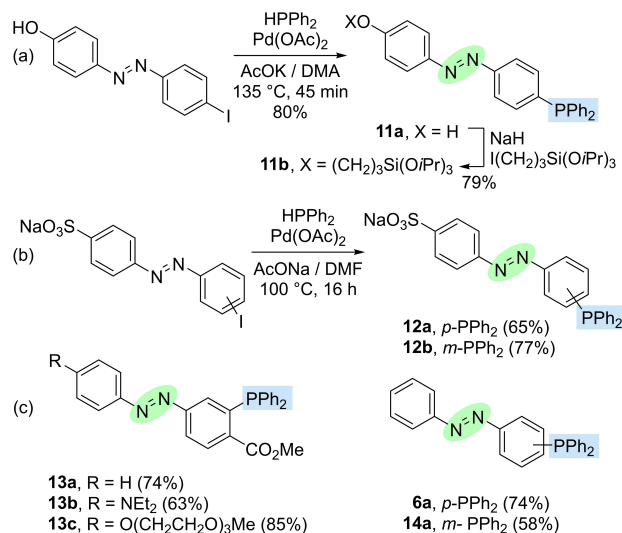
Scheme 4. Synthesis by lithiation/phosphination of iodo- or bromo-azobenzenes.

display three azobenzene units on phosphorus have been prepared by halogen-lithium exchange, followed by reaction with PCl_3 (Scheme 4c).^[15c,18] Alternatively, lithiated azobenzenes have been reacted with ClP(S)Ph_2 and the corresponding phosphines **10** have been obtained then by desulfuration with tributylphosphine (Scheme 5).^[19]

Palladium(II)-promoted couplings of iodo-azobenzenes with secondary phosphines (Ar_2PH) are typified in Scheme 6 by the synthesis of phosphines bearing hydroxyl (or alkoxy) and sulfonate functions, reported by Corriu^[20] and Monflier^[21] respectively (Scheme 6a–b). These reactions were performed by heating the substrates mixtures at 100–135 °C in the presence of Pd(OAc)_2 . The same strategy and analogous conditions allowed the synthesis of the ester-functionalized phosphines **13**^[22] and the parent *para*- and *meta*-phosphines **6a** and **14a**^[18a] (Scheme 6c). These few examples show that, despite the rather harsh conditions, the method tolerates the diazo unit as well as the presence of functional groups. It tolerates also a degree of steric hindrance, since the *ortho*-substituted phosphines **13** could be obtained in good yields.

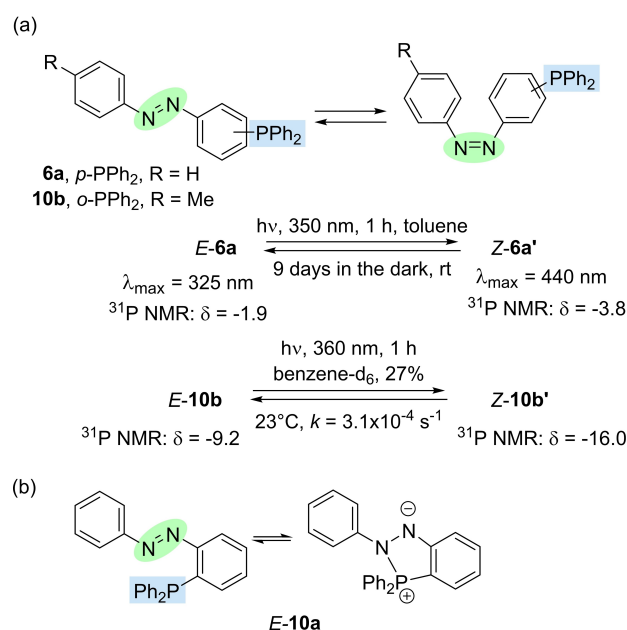


Scheme 5. Two-step synthesis from lithiated azobenzenes and $\text{Ph}_2\text{P(S)Cl}$.



Scheme 6. Synthesis by Pd(II)-promoted coupling of iodoazobenzenes.

The photochemical behavior of azobenzene-derived phosphines is illustrated in Scheme 7 by the *E/Z* reversible isomerization of phosphines **6a** and **10b**.^[18a,19a] These reactions have been monitored by UV-vis and ^{31}P NMR spectroscopy. Thus, when a toluene solution of *E*-**6a** was irradiated at 350 nm in toluene, UV monitoring showed a decrease of the 325 nm band typical of the *E*-isomer ($\pi \rightarrow \pi^*$ transition), with concomitant increase of the 440 nm band characteristic of the *Z*-isomer ($n \rightarrow \pi^*$ transition). After 1 h an approximately 1:4 *E:Z* mixture was obtained. The thermal back *Z*→*E* isomerization proved to be slow, a ~1:1 ratio of the two



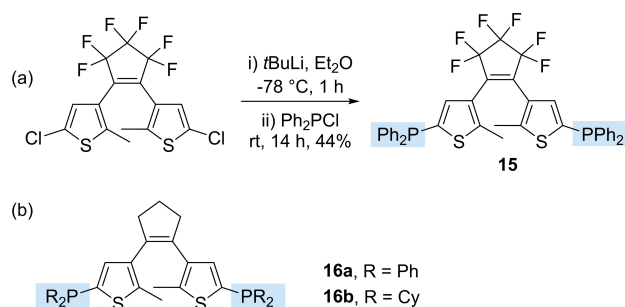
Scheme 7. Representative photoswitch of azobenzene-derived phosphines.

isomers **6a/6a'** being observed after 38 h in the dark at 25 °C.^[18a]

An analogous behavior has been observed for the *o*-phosphine **10b** that bears a *p*-tolyl group (R=Me) on the diazo unit (Scheme 7a). However, the unsubstituted *o*-phosphine **10a** (R=H, Scheme 7b) does not undergo photoisomerization under analogous conditions. This phosphine is locked indeed in its *E*-form as a result of the equilibrium between the P(III) and the inner phosphonium salt forms (Scheme 7b, right).^[19a] As far as we know, this is the only example in which photoisomerization of a trivalent azobenzene-phosphine does not proceed.

2.2. Dithienylcyclopentene derived mono- and diphosphines

Besides azobenzenes, the most widely studied photochromic backbones are 1,2-dithienylethenes (DTE). They are P-type chromophores that interconvert reversibly between “ring-opened” and “ring-closed” forms by light induced C–C bond formation/cleavage (Scheme 1b). Compounds of this class generally display good thermal stability of both forms and tolerate a large number of switching cycles (high fatigue



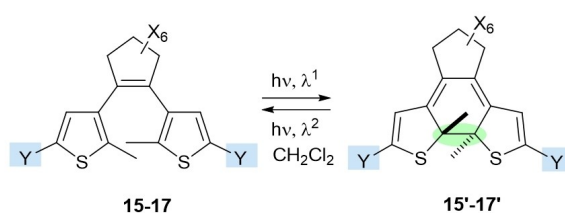
Scheme 8. Synthesis of dithienylethene-based diphosphines.

resistance). Furthermore, the two isomers have markedly different three-dimensional geometries, conformational freedom and physicochemical properties.

In 2005, Branda disclosed the first examples of trivalent phosphines displaying a dithienylethene backbone.^[23] Starting from 1,2-*bis*-(5'-chloro-2'-methylthienyl)perfluoro-cyclopentene, an halogen-lithium exchange and subsequent reaction with Ph₂P-Cl, led to diphosphine **15**. The phosphorus functions are attached to positions 5' of the two thiophene units (Scheme 8a). Later on, Liu^[24] applied the same method to the synthesis of the related C₂-symmetric diphosphines **16a,b** (Scheme 8b) from a non-fluorinated dithienylcyclopentene dichloride. The corresponding oxides, sulfides and selenides have been described as well.

The photocyclizations of fluorinated and non-fluorinated phosphines of this series have been investigated independently (Scheme 9). Diphosphine **15** undergoes ring closure under irradiation at 313 nm in CH₂Cl₂, giving a 20:80 ratio of the two isomers at the photostationary state.^[23] The solution changed from colorless to deep purple, since the closed isomer **15'** shows an absorption band at λ_{max}=570 nm. The reverse ring-opening process occurred under irradiation at λ > 434 nm. Most noteworthy, the photoisomerization cycle could be performed several times without significant degradation. To get insights on the effects of the photoisomerization on the electronic properties of **15/15'**, the authors measured ¹J(⁷⁷Se–³¹P) coupling constants in the corresponding *bis*-selenides. The results showed that the open form of the phosphine (¹J_{P–Se}=744 Hz) is significantly more electron-rich than the corresponding closed isomer (¹J_{P–Se}=756 Hz).

The non-fluorinated dithienylethene diphosphines **16a,b** gave cyclization/ring opening reactions under irradiation at 254 nm and 510 nm respectively. The UV-vis spectra of the open forms **16a,b** (Y=PPh₂ and Y=PCy₂) show absorption bands at λ_{max}=228 and 233 nm, while the red-colored closed forms **16a',b'** display red-shifted absorption bands at 505 and



Comp	X	Y	³¹ P NMR δ (ppm), J (Hz)	λ ¹	λ ²	PSS	Ref
15/15'	F	PPh ₂	-18.7/-8.3	313	>434	20:80 ^[c]	[23]
17	F	P(Se)Ph ₂	22.4/27.0 <i>J</i> _{P–Se} =744/756	313	>434	45:55 ^[c]	[23]
16a/16a'	H	PPh ₂	-20.0	254 ^[a]	510 ^[b]	70:30 ^[d]	[24]
16b/16b'	H	PCy ₂	-9.1	254	510	73:27 ^[d]	[24]

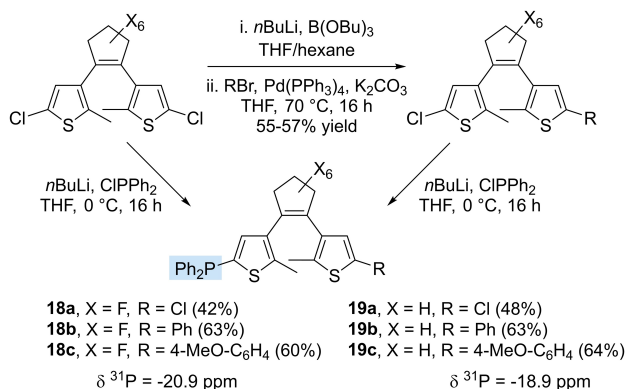
[a] Quantum yield Φ = 0.14; [b] Φ = 0.84; [c] Ratio determined by ¹H NMR; [d] Ratio determined by HPLC

Scheme 9. Photoisomerization of dithienylcyclopentene-derived diphosphines and a diphosphine *bis*-selenide.

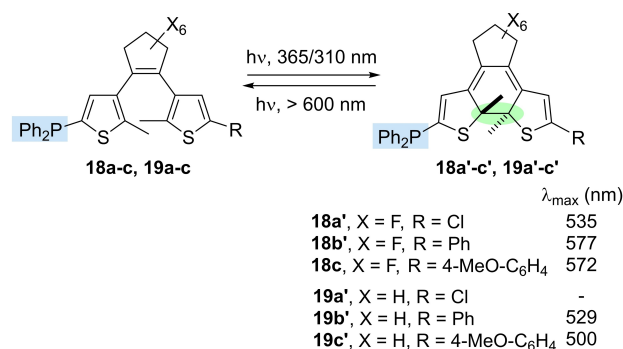
497 nm respectively. Thus, compared to diphosphine **15'**, the non-fluorinated diphosphines **16a',b'** display the red-shifted absorption bands at significantly lower wavelengths ($\Delta\delta = -65$ nm).

In 2015, Wass, Scarso *et al.*^[25] have reported on two series of mono-phosphines, **18a–c** and **19a–c**, with fluorinated and non-fluorinated dithienylcyclopentene backbones respectively. These compounds feature chlorine, phenyl and anisyl substituents on the second thiophene unit (Scheme 10). They were obtained from the corresponding thienyl chlorides by a lithiation/phosphination sequence. The ³¹P NMR spectra of the corresponding selenides showed that phosphines with fluorinated backbones have lower electron-donating ability (e.g. ¹J_{P–Se} = 744 Hz for **18c** vs 737 Hz for **19c**), while the nature of the R substituent on the remote thiophene unit does not make substantial difference.

The photoinduced cyclization took place under UV irradiation at 365 nm for the aryl-substituted compounds **18b,c** and **19b,c** (R = aryls), while the chloro-substituted phosphines **18a** and **19a** were irradiated at 310 nm to generate their closed forms. The reverse ring-opening reaction took place under irradiation at $\lambda > 600$ nm. As shown in Scheme 11, the absorption wavelengths of the cyclized isomers **18'** and **19'** in the visible region are highly dependent on their respective substitution patterns. Thus, solutions of **18b'** and **18c'** are blue-colored, while **19b'** and **19c'** give



Scheme 10. Synthesis of dithienylcyclopentene derived mono-phosphines.



Scheme 11. Photocyclization conditions and absorption maxima of the closed forms **18'** and **19'**.

red solutions and **19a'** a yellow-orange one. This last compound showed an increased absorption in the range 450–300 nm, but did not display defined λ_{\max} values.

In this series also, ring closure decreases the σ -donating ability of the phosphines, as shown by the increased ¹J_{P–Se} coupling constants in the corresponding selenides after cyclization (e.g. ¹J_{P–Se} = 742 Hz for **18a** and ¹J_{P–Se} = 757 Hz for **18a'**; ¹J_{P–Se} = 737 Hz for **19a** and ¹J_{P–Se} = 747 Hz for **19a'**).

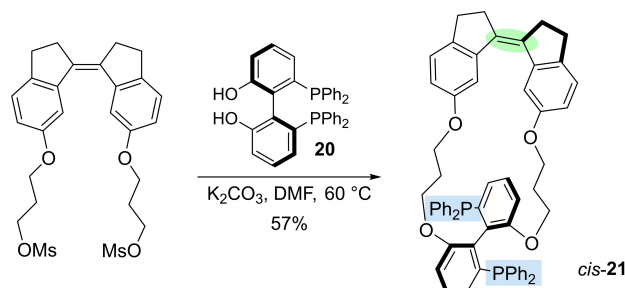
2.3. Biindane derived diphosphines

Only three recent literature reports relate to the synthesis of biindane-derived phosphines from suitably functionalized biindanes.

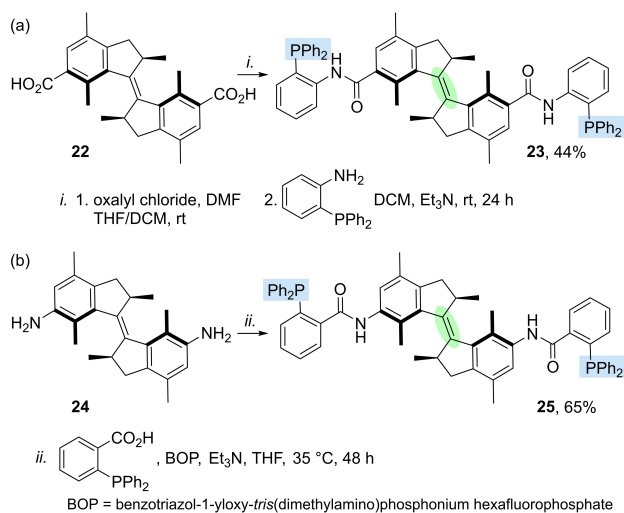
In 2014, Widenhoefer, Boulatov and Craig have prepared the macrocyclic diphosphine **21** by O-alkylation of the (*S*)-diphosphine **20**, using a biindane-derived *bis*-mesylate (Scheme 12).^[26] The diphosphine has been used then as chiral ligand in palladium-promoted Heck reactions that will be discussed in section 4.3.1 hereafter.

The two other reports on biindane-derived diphosphines are from the Feringa group. In 2015, the group disclosed the synthesis of diphosphines *trans*-**23** and *trans*-**25** in which amide functions connect a biindane scaffold to diphenylphosphino-aryl groups (Scheme 13).^[27] The phosphorus function of *trans*-**23** has been introduced by amidation of the enantioenriched biindane-carboxylic acid *trans*-**22** with *ortho*-diphenylphosphino-aniline. On the other hand, the optically pure amino-biindane *trans*-**24**^[28] has been converted into diphosphine *trans*-**25** by coupling with *ortho*-diphenylphosphino-benzoic acid in the presence of BOP. The photochemical and thermal isomerization of *trans*-**23** will be discussed later in the context of its uses in catalysis (see § 4.3.2). The isomerization of *trans*-**25** under irradiation at 312 nm (–15 °C in THF) led to only 7% conversion into the corresponding *cis*-isomer and, therefore, this phosphine was not investigated further.

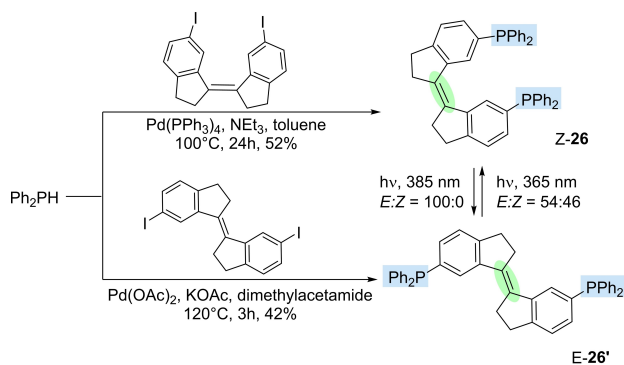
Finally, in 2020, B. L. Feringa reported on the synthesis of the parent *Z*- and *E*-biindane-derived diphosphines **26** and **26'** *via* palladium-promoted couplings of the corresponding 6,6'-diiodobiindanes with Ph₂PH (Scheme 14).^[29] The two compounds have distinct absorption spectra with $\lambda_{\max} = 356$ nm for *Z*-**26** and $\lambda_{\max} = 338$ and 356 nm for *E*-**26'**. *Z*→*E*



Scheme 12. Synthesis of a biindane-derived macrocyclic diphosphine.



Scheme 13. Synthesis of biindane-based diphosphines.



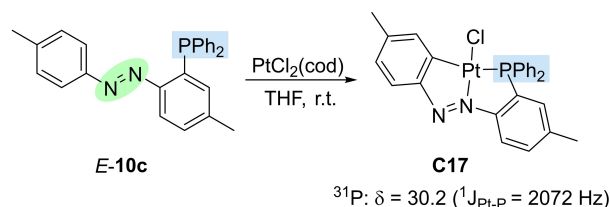
Scheme 14. Synthesis of the biindane derived diphosphines 26 and 26' via Pd-promoted phosphination.

conversion takes place quantitatively under irradiation at 385 nm and the reverse E \rightarrow Z isomerization under irradiation in benzene at 365 nm (E/Z 54/46 mixture at the photostationary state). From ^{31}P NMR experiments on the corresponding selenides, it was demonstrated that the donor properties of phosphorus are almost identical for the two isomers ($^1J_{\text{P-Se}} = 364$ Hz).

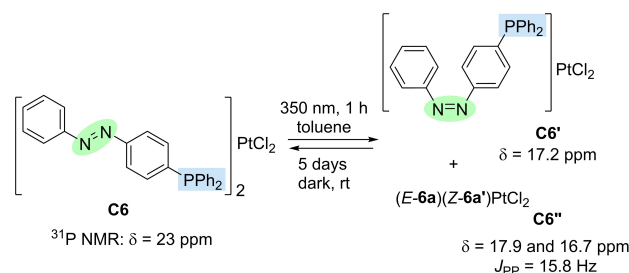
3. Transition metal complexes

3.1. Complexation of preformed phosphines

Most commonly, transition metal complexes of azobenzene, DTE and biindane derived phosphines are obtained by coordination of the preformed phosphine to a suitable metal precursor. The known examples of metal complexes obtained by this method are listed in Table 1.



Scheme 15. An example of platinumacyclic complex.



Scheme 16. Photoisomerization of the platinum(II) complex C6.

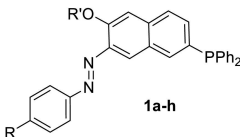
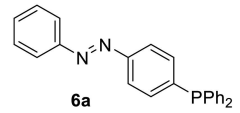
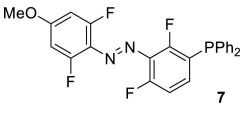
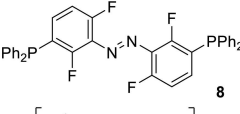
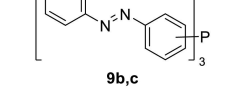
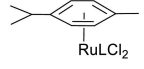
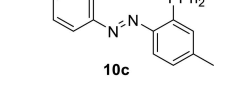
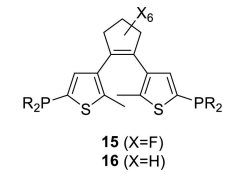
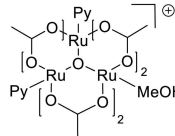
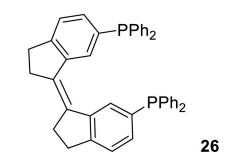
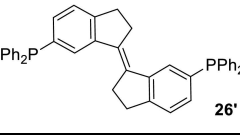
3.1.1. Azobenzenes

For all the examples of azobenzene derivatives quoted in the Table, coordination of phosphorus to a transition metal takes place under standard conditions and does not induce major structural changes of the ligands. A divergent behaviour has been reported however for ligand *E-10c* in its reaction with $\text{PtCl}_2(\text{cod})$. In this case, the reaction leads to the platinumacyclic species C17 by concomitant coordination of phosphorus and nitrogen and metalation of the aryl ring (Scheme 15).^[33] The molecular structure of the final product has been ascertained by X-ray diffraction studies.

In most instances, in the azobenzene series, coordination does not influence significantly neither the E \rightarrow Z photoisomerization nor the reverse thermal process. Thus, coordination of *E-6a* to Pt(II), generates the *cis-(E-6a)* $_2$ PtCl $_2$ complex C6 that undergoes E \rightarrow Z isomerization under irradiation at 350 nm in toluene for 1 h. The resulting mixture contains the (Z-6a') $_2$ PtCl $_2$ complex C6' and a complex featuring both an *E*- and a *Z*-ligand (C6''), together with traces of the starting material C6. The mixture undergoes slow back isomerization in the dark at room temperature (Scheme 16)^[18a] The same holds for the (*p*-cymene)Ru(9)Cl $_2$ complex C9 displayed in Table 1: the half-life time of the *Z*-isomer is roughly identical to that of the corresponding phosphine 9c (115 min at 55 °C).^[18b]

3.1.2. Dithienylcyclopentenes

Concerning dithienylcyclopentene based diphosphines, coordination to gold,^[23,34,36] palladium^[34] and ruthenium^[35] has been reported.

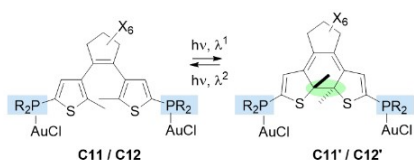
Phosphine	Metal complex	Metal precursor	Yield	ref	
 1a-h	C1	<i>trans</i> -L ₂ PdCl ₂ ^[a]	Na ₂ PdCl ₄	56–72%	[30]
	C2	<i>cis</i> -L ₂ PtCl ₂ (R'=H, Ac, R=Me, NMe ₂)	Na ₂ PtCl ₄	55–59%	[30]
	C3	LAuCl ^[b] (R'=H, Ac; R=Me, NMe ₂ , NO ₂)	NaAuCl ₄ /(HOCH ₂ CH ₂) ₂ S	59–85%	[31]
	C4	LM(CO) ₅ (M=Cr, Mo, W)	(CO) ₅ M(MeCN)	30–72%	[32]
	C5	L ₂ Mo(CO) ₄ (R'=H, R=H, Me, Et, <i>i</i> Pr, <i>t</i> Bu; R'=Ac, ^b R'=Me)	(CO) ₄ Mo(piperidine) ₂	42–75%	[32]
 6a	C6	<i>cis</i> -L ₂ PtCl ₂	Cl ₂ Pt(COD)	–	[18a]
 7	C7	LAuCl	(Me ₂ S)AuCl	75%	[17]
 8	C8	L(AuCl) ₂	(Me ₂ S)AuCl	82%	[17]
 9b,c	C9		Ru[(<i>p</i> -Cymene)Cl] ₂	90–95%	[18b]
 10c	C10	LW(CO) ₅	W(CO) ₅ (THF)	75%	[33]
 15 (X=F) 16 (X=H)	C11	L(AuCl) ₂ L = 15, R=Ph	AuCl(tetrahydrothiophene)	18%	[23]
	C12	L = 16a, R=Ph L = 16b, R=Cy	(Me ₂ S)AuCl (Me ₂ S)AuCl	89%	[34] [34]
	C13	L(PdCl ₂) ₂ L = 16a, R=Ph	PdCl ₂ (PhCN) ₂	85%	[34]
	C14	L[Ru ₃ (O)(OAc) ₆ Py ₂] ⁺ + PF ₆ ⁻		80%	[35]
	C15	L[Ru ₃ (O)(OAc) ₆ Py ₂] ₂ ²⁺ + (PF ₆) ₂ ⁻ L = 16a, R=Ph		82%	[35]
 26	C16	<i>trans</i> -L(PdCl ₂)	Pd(MeCN) ₂ Cl ₂	78%	[29]
 26'	C16'	[<i>trans</i> -L(PdCl ₂) ₂]	Pd(MeCN) ₂ Cl ₂	74%	[29]

[a] For R'=H the ligands adopt mainly keto-hydrazone tautomeric forms. [b] For R'=COMe, the complex was obtained by O-acylation of the corresponding OH-functionalized L₂Mo(CO)₄ complex.

The bis-gold complexes **C11**, **C12a** and **C12b** that contain diphosphines **15** (X=F, PR₂=PCy₂), **16a** and **16b** (X=H, PR₂=PPh₂ and PCy₂) respectively, undergo reversible conversion between ring-opened and ring-closed isomers under irradiation with 302 nm UV light and >400 nm visible light (Scheme 17). The red-colored closed forms **C11'**, **C12a'** and **C12b'** have absorption maxima at 565, 517 and 503 nm respectively, that is slightly

blue-shifted for **C11'** and red-shifted for **C12a'** and **C12b'**, with respect to the corresponding phosphines ($\lambda_{\text{max}}=570, 505$ and 497 nm respectively).

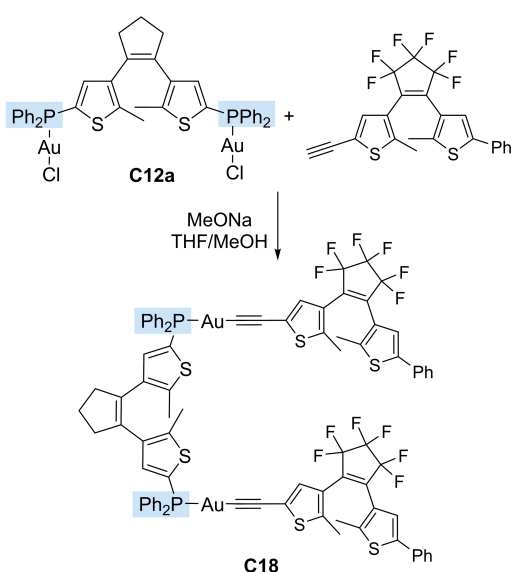
In further studies, the bimetallic gold chloride complex **C12a** has been converted into a bis-gold-acetylide complex featuring two additional dithienylcyclopentene units (**C18**, Scheme 18).^[36] The aim was to induce multiple photochromic



Comp	X	PR ₂	λ _{max}	Comp	λ _{max}	λ ¹	λ ²	Ref
C11	F	PPh ₂	-	C11'	565	313	>434 ^[a]	[23]
C12a	H	PPh ₂	229	C12a'	517	302	>400	[34]
C12b	H	PCy ₂	232	C12b'	503	302	>400	[34]

[a] The PSS consists in a **C11**:**C11'** 40:60 mixture in CH₂Cl₂.

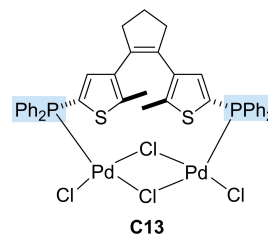
Scheme 17. Photoisomerization and absorption maxima for the gold complexes **C11** and **C12**.



Scheme 18. Synthesis of multi-dithienylethenes from the bimetallic gold complex **C12a**.

reactions in a single molecule. Thanks to the gold spacers, the two non-equivalent photochromic switches of **C18** operate independently. Thus, the closed forms are obtained in a stepwise manner, under irradiation at 365 nm for the F₆-cyclopentene units and under irradiation at 254 nm for the cyclopentene unit.

The examples given in Scheme 17, but also analogous studies on ruthenium complexes,^[35] suggest that coordination of dithienylethene based phosphines to transition metals may not change significantly the photoswitch process. In other instances the nature and the electronic properties of the ancillary ligands on the metal may modulate the photoswitch properties of the complexes (see § 3.2 hereafter). Finally, it has been found that the bimetallic, chloride bridged palladium complex **C13** (Scheme 19) does not undergo photoisomerization because of the geometrical constraints of its macrocyclic structure that enforces a long C–C



Scheme 19. A non-photoactive palladium complex.

distance between the reactive carbons (4.2 Å). It also enforces a parallel conformation of the two thiophene units, while an anti-parallel orientation is required for the symmetry-allowed conrotatory electrocyclozation of the DTE moiety.^[34]

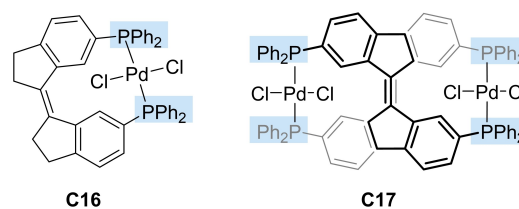
3.1.3. Biindanes

In the biindane series, transition metal complexes have been isolated only recently.^[29] Diphosphines **Z-26** and **E-26'** (see Scheme 14) have been coordinated to palladium dichloride in separate experiments by reacting the free ligands with Pd (MeCN)Cl₂. The *Z*-isomer of the ligand generated the mono-metallic *trans*-configured chelated complex **C16**, while the *E*-ligand **26'** afforded the dimeric complex **C17** (Scheme 20). These complexes do not undergo photoisomerization, because of their geometrical constraints.

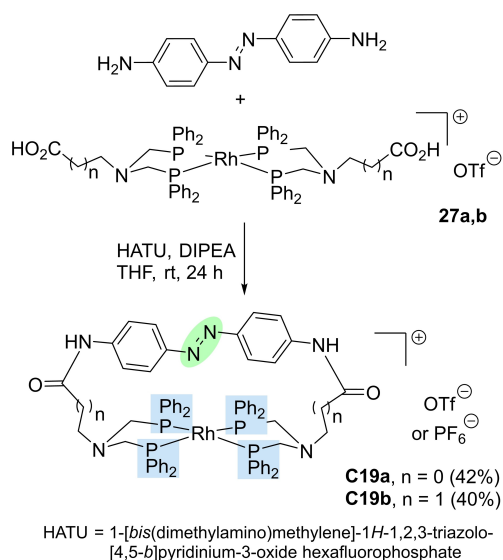
3.2. Building of photoswitchable phosphines in the coordination sphere of a metal

An alternative to complexation of preformed ligands consists in building the photoswitchable ligands directly in the coordination sphere of the metal. This approach is illustrated in Scheme 21^[37] by the synthesis of the macrocyclic rhodium (I) complexes **C19a,b**. These complexes are formed by reacting the *p,p'*-diaminoazobenzene in Scheme 21 with the carboxylic acid functions of the bis-phosphine rhodium complexes **27a,b**. The amidation reaction creates a macrocyclic tetradentate ligand that incorporates an azobenzene bridging unit.

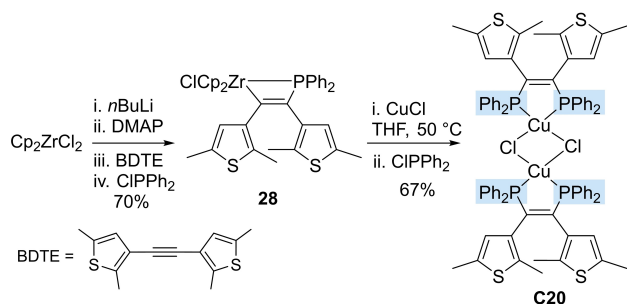
A second example is the synthesis of the bimetallic copper(I)-complex **C20**, in Scheme 22.^[38] The key intermedi-



Scheme 20. Mono- and bimetallic Pd(II) complexes of biindane-derived diphosphines.



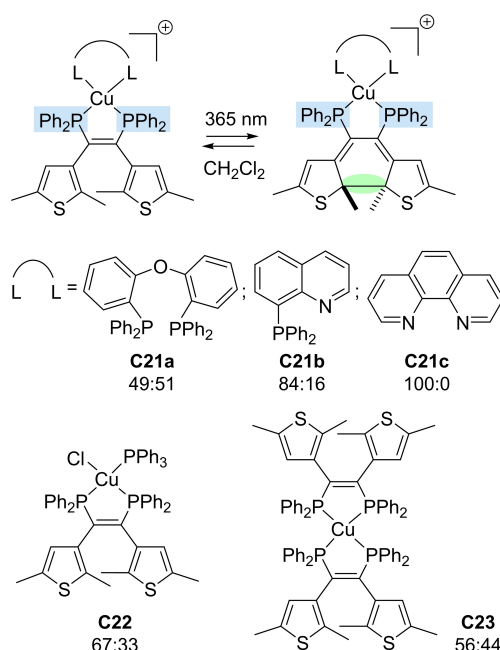
Scheme 21. Synthesis of macrocyclic Rh(I) complexes.



Scheme 22. Synthesis of a copper-complex of DTE-based diphosphines.

ate is the phosphino-dithienylethene-zirconacycle **28** that undergoes a zirconium-copper transmetalation, followed by phosphination of the resulting copper intermediate with $\text{Ph}_2\text{P}(\text{Cl})$. It must be noticed that the diphosphine ligands in complex **C20** belong to a distinct series of dithienylethene-diphosphines with respect to the previous examples: here, the phosphorus functions are attached to the central olefinic bond, instead of being attached to the thiophene units.

Starting from the bimetallic complex **C20**, ligand exchange reactions gave access to the copper complexes **C21** (Scheme 23) that display either phosphorus or nitrogen ligands. This homogeneous series of metal complexes has allowed comparative studies of their photochemical behavior. These studies have highlighted a crucial effect of the ancillary ligands on the ratio between open and cyclized forms at the PSS, under irradiation at 365 nm (Scheme 23).^[38] Thus, it has been shown that changing one of the coordinating phosphorus groups in **C21a**, by either a chloride (as in **C22**) or a pyridine-type ligand (as in **C21b**) decreases the amount of cyclized forms at the photostationary state, from 51% to 33% and 16% respectively. Moreover, isomerization was totally prevented in **C21c** that displays a 1,10-phenan-



Scheme 23. Photoisomerization of a series of copper complexes of dithienylethene-diphosphines. Ratios of open:closed forms at the photostationary states (365 nm).

tholine as the ancillary ligand. DFT calculations have suggested that the decreased photoreactivity of the pyridine-ligated complexes **C21b** and **C21c** might result from localization of their LUMOs orbitals mainly on the quinoline and 1,10-phenanthroline ligands. Complex **C21a** showed photocycloreversion under irradiation at $\lambda > 500$ nm, with good reversibility after up to eight photochromic cycles.

As a conclusion it may be recalled that, in many instances, coordination of photoswitchable phosphines to transition metals does not change significantly their photoswitch properties. However, in some cases, either geometrical constraints or electronic effects of ancillary ligands may modulate their photochemical behaviors. To fully enlighten these effects, more extended, systematic studies on homogeneous series are still required.

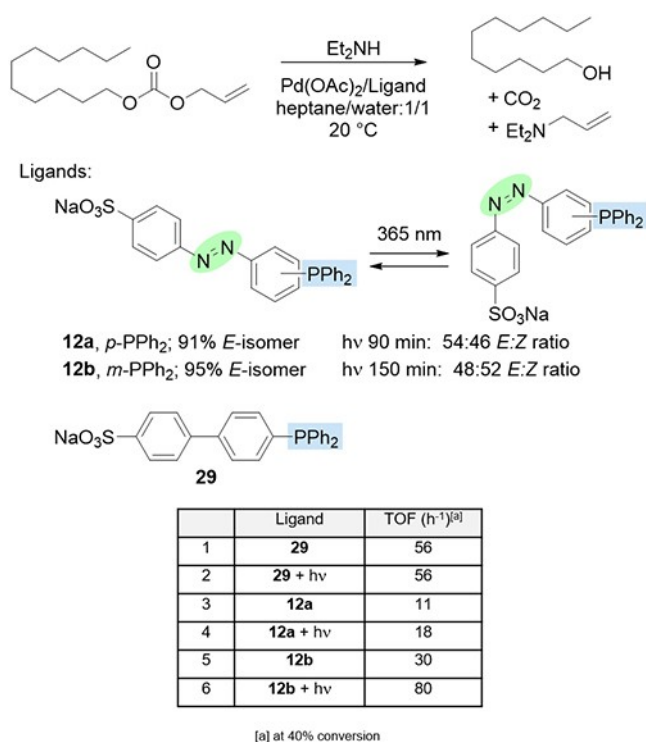
4. Catalytic applications

In the following sections we will summarize literature reports where significant effects of photoswitch on the catalytic activity of transition metal complexes have been highlighted. In a few additional reports the catalytic activity has been investigated, but the effects of photoswitch haven't been mentioned.^[14,30,34]

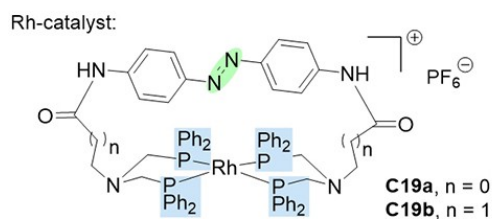
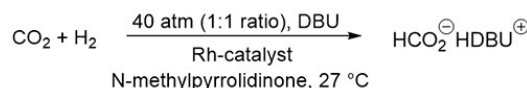
4.1. Catalysts derived from azobenzene based mono- and diphosphines

4.1.1. Palladium-promoted decarboxylation of allylic carbonates

The water soluble, sulfonated azobenzene derived phosphines **E-12a,b** undergo isomerization under irradiation at 365 nm, leading to 54:46 and 48:52 *E/Z* mixtures respectively at the photostationary state. The mixtures give back the initial *E/Z* ratios after one night at room temperature in the dark, or after 10 min under daylight. These phosphines have been used as amphiphilic ligands in the Pd(II)-promoted decarboxylation of allyl undecyl carbonate with diethylamine. The reactions were run both in the dark and under irradiation, and parallel experiments have been conducted with the analogous biphenyl-phosphine **29**, for comparison purposes (Scheme 24).^[21] Overall, without UV irradiation, the presence of the diazo function has a detrimental effect on the reaction rate (entries 1,3,5 in Scheme 24). However, upon irradiation (entries 4, 6), the reaction rate increased. Especially, with **12b**, an increase of the rate by more than 2.5-folds led to the best turnover frequency in this series (80 h⁻¹). It has been shown that phosphines **12a** and **12b** form aggregates in water (decreased surface tension). Therefore, the positive effect of the *E*→*Z* isomerization on the reaction rate has been assigned to the formation of new aggregates that possibly solubilize the substrates in a more efficient way.



Scheme 24. Palladium-promoted decarboxylation of allylic carbonates.



	Catalyst	TOF (h ⁻¹)
1	C19a	11±2
2	C19a + hv, λ _{max} 365 nm	16±2
3	C19b	17±0.2
4	C19b + hv, λ _{max} 365 nm	18±0.2

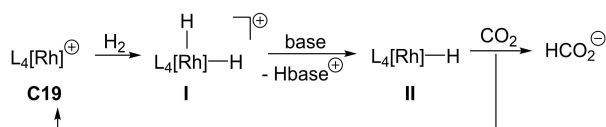
Scheme 25. Rhodium(I)-promoted hydrogenation of CO₂.

These studies have afforded the first example of organo-metallic catalysis in biphasic media, regulated and stimulated by the *in situ* photoisomerization of the ligands.

4.1.2. Rhodium-promoted hydrogenation of CO₂

The macrocyclic rhodium(I) complexes **C19a** and **C19b** feature a tetradentate phosphine ligand and an azobenzene moiety spanning the metal centre. The two complexes display one and two carbon units respectively (n=0,1) in the chains tethering the phosphorus functions. They have been specifically designed to investigate the impact of geometry changes on the catalytic hydrogenation of CO₂ (Scheme 25).^[37] Irradiation of these complexes at 375 nm converts *E*-**C19** into their *Z*-isomers **C19a'** and **C19b'**, as shown by UV and NMR monitoring. The reverse isomerization takes place slowly (k=9.9×10⁻³ and 8.7×10⁻³ min⁻¹ for **C19a'** and **C19b'** respectively), with complete relaxation after 6 to 8 hours. (For comparison, the *Z*→*E* isomerization of the 4,4'-diaminoazobenzene precursor in Scheme 21 takes place in 15 min). The slowdown is likely due to the restricted flexibility of the macrocyclic complexes.

The hydrogenation experiments have been carried out in a stainless reactor with a sapphire window, under 40 atm of a 1:1 CO₂/H₂ mixture, both in the dark and under continuous irradiation. The largest macrocycle **C19b** (n=1), displayed the same reaction rate under both conditions. On the contrary, irradiation of complex **C19a** (n=0) led to a more active catalyst, giving a 40% rate enhancement. In depth theoretical, kinetic and thermodynamic studies of the individual catalytic steps (Scheme 26) showed that the reaction rates do not correlate, in a direct way, with the extent of geometrical changes in the outer coordination sphere that are induced by irradiation. They do not correlate either with the rates of the oxidative addition of H₂ on complexes **C19**. Finally, it is postulated that the reaction rate should be

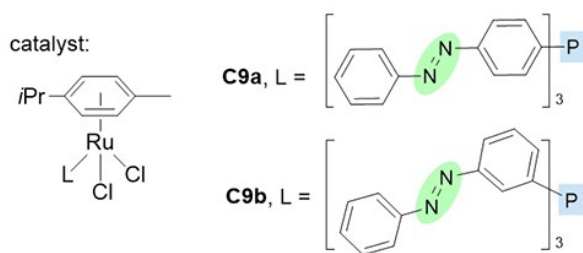
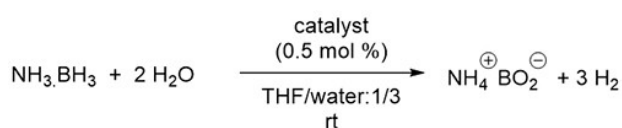
Scheme 26. Key steps of the rhodium-promoted hydrogenation of CO₂.

affected by small changes of the P–Rh–P bite-angles that modulate critically the hydricity (hydride transfer ability) of the rhodium monohydride intermediate II in Scheme 27.

This study suggests that geometrical changes of a remote azobenzene moiety, in the outer coordination sphere of a transition metal, can regulate reaction rates by subtle changes of the bite angles at the metal center.

4.1.3. Ruthenium-promoted release of dihydrogen from ammonia-borane

Ammonia-boranes, NH₃–BH₃, provide promising materials for hydrogen storage and subsequent release under metal catalysis. Thus, the (*p*-cymene)ruthenium dichloride complexes **C9** have been considered as catalysts for the controlled release of hydrogen from these adducts (Scheme 27).^[18b] Complexes **C9** bear the monodentate *tris* (azobenzene)phosphines **9** as photoswitchable ligands. The three azobenzene units of each ligand adopt mainly the most stable *E*-forms (*EEE*-isomers), but small amounts of the isomeric *EEZ*-ligands may be present, with up to a 25% amount for **C9b**. Irradiation of these samples at 324 nm, for 30 min in CD₃CN, induces *E*→*Z* isomerization. The reverse *Z*



	Catalyst	Conversion rate ^[a]	
		t = 50 min	t = 100 min
1	C9a	30%	45%
2	C9a + hv	60%	100%
3	C9b	35%	50%
4	C9b + hv	65%	95%

[a] approximate values from reaction profiles in ref.^[18b]

Scheme 27. Ruthenium-promoted H₂ release from ammonia-borane.

to *E* isomerization takes place at 65 °C, with *t*_{1/2} = 115 and 144 min for **C9a** and **C9b**, respectively.

The ruthenium complexes **C9** enabled the hydrolytic generation of hydrogen from ammonia-borane at a 0.5 mol % catalyst loading, in a THF-water mixture. The release of H₂ was monitored from pressure evolution, both in the dark and under continuous irradiation (immersion lamp, 125 W, 365 nm). For both complexes **C9**, the catalytic activity was much higher under irradiation, compared to dark conditions. In an additional experiment, with catalyst **C9b**, irradiation and no-irradiation periods were alternated. The reaction profiles clearly showed alternating slopes with different reaction rates.

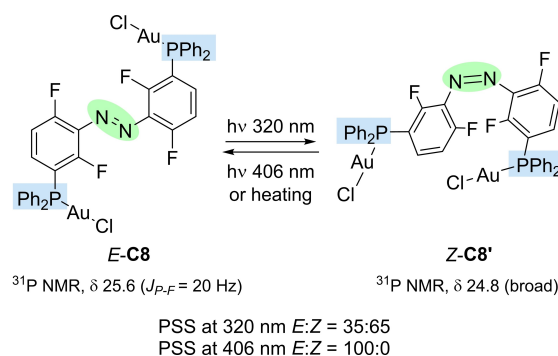
After several control experiments, including comparison with the model (Ph₃P)Ru(*p*-cymene)Cl₂ complex, the positive effect of UV irradiation has been assigned to the increased steric bulk of the *Z*-configured phosphorus ligands (increased cone angle). However, the effect couldn't be fully rationalized, mainly due to lack of mechanistic knowledge on this reaction.

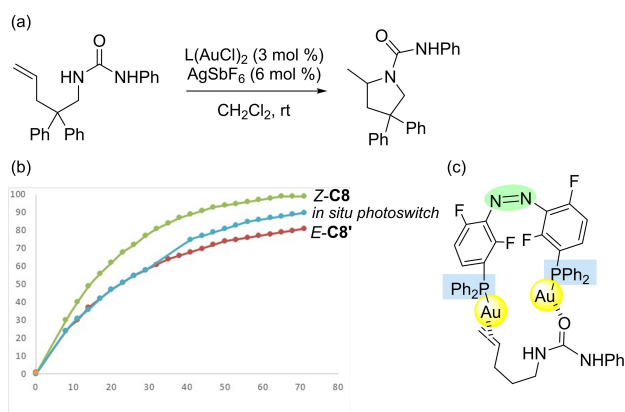
Overall, the phosphine-ruthenium complexes **C9** proved to be suitable photoswitchable hydrogen release catalysts. Interestingly, complexes **C9** perform better than analogous ruthenium complexes with azobenzene-derived bipyridine ligands that isomerize less efficiently and suffer dissociation under irradiation.

4.1.4. Gold(I)-promoted intramolecular hydroaminations

Our group has reported recently on photoswitchable bimetallic gold complexes of azobenzene-derived diphosphines and their use in the intramolecular hydroamination of *N*-alkenylureas.^[17]

The bimetallic complex *E*-**C8** undergoes fast photoisomerization under irradiation at 320 nm in MeCN (Scheme 28). As shown by UV monitoring, the photostationary state is reached after 60 seconds, with an *E*:*Z* ratio = 35:65. The reverse process takes place either under irradiation at 406 nm (240 sec) or under thermal conditions, with a *t*_{1/2} = 278 h at 60 °C. The fluorine substituents on the azobenzene core make the *Z*-form stable enough to be isolated,

Scheme 28. Photoisomerization of the bimetallic gold complex **C8**.



Scheme 29. (a) Hydroamination reactions promoted by the bimetallic gold complexes **C8**; (b) Kinetic profiles; (c) Postulated bimetallic activation of the substrate.

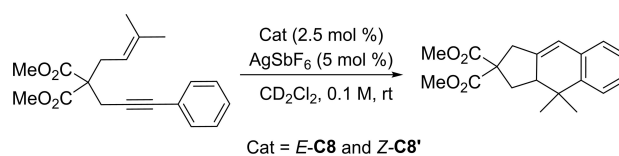
characterized by X-ray diffraction, and used then in the catalytic tests shown in Scheme 29.

The active cationic catalysts were generated from $E-C8$ and $Z-C8'$ separately, by removing chlorides with $AgSbF_6$. The reaction course was monitored by *in situ* 1H NMR (CD_2Cl_2 solutions) with automatic recording. Both Z - and E -catalysts displayed good catalytic activity in the intramolecular hydroamination reaction, with the Z -isomer giving significantly higher reaction rate and conversion (Scheme 29). Also, an *in situ* switch experiment was carried out. The experiment started with catalyst $E-C8$ and then, after 30 min (at ~55% conversion rate), the mixture was irradiated at 320 nm for 10 min to generate $Z-C8'$. Irradiation led to acceleration of the hydroamination reaction, the conversion rates approaching those obtained with preformed $Z-C8'$ under analogous conditions.

After several control experiments, including comparison of **C8** with the azobenzene derived monometallic gold complex **C7** (see Table 1), the higher catalytic activity of the Z -isomer **C8'** has been assigned to synergistic cooperative effects between the two metal centers. Indeed a bimetallic activation of the substrate can be postulated (Scheme 29c), that is expected to be enhanced with Z -configured catalysts, owing to the shorter distance between the two metals.

In parallel, the same gold complexes **C8** have been used as pre-catalysts in the enyne cycloisomerization reaction shown in Scheme 30. In this reaction where synergistic effects between the metals are not expected, the Z - and E -forms of the catalyst show the same kinetic profiles.

Overall, these results validate the working hypothesis on which the study had been built initially, *i.e.* that bimetallic complexes are especially suited to demonstrate photoswitch phenomena in catalysis, as far as they may enable ON-OFF switch of cooperative effects between the two metals. Beyond the external control of catalytic reactions, bimetallic complexes of this class might also afford unprecedented probes to highlight cooperative effects in bimetallic processes.



Scheme 30. Enyne cycloisomerization promoted by the bimetallic gold complexes **C8**.

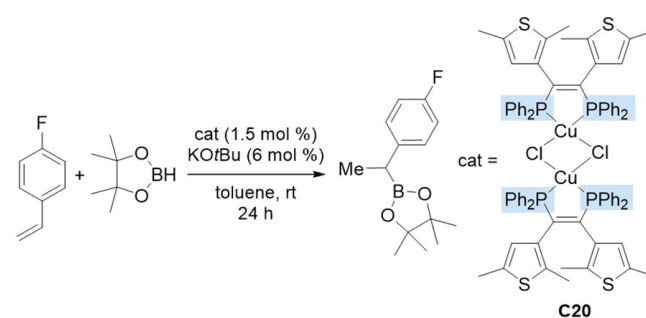
4.2. Catalysts based on dithienylethene diphosphines

As far as we know, only one example of light-induced modulation of the catalytic activity of metal complexes featuring dithienylethene-phosphines has been reported so far.

4.2.1. Copper(II)-promoted hydroboration of styrenes

The bimetallic copper complex **C20** has been used as pre-catalyst in the hydroboration of 4-fluorostyrene (Scheme 31).^[38] The active catalyst was generated *in situ* from **C20**, by addition of potassium *tert*-butoxide in the presence of pinacolborane. Hydroboration was performed first in the dark, then, in a second experiment, the active catalyst was irradiated for 20 minutes at 365 nm before addition of the substrate. Under irradiation, the orange catalyst solution turned red, as expected. The hydroboration reactions were monitored by gas chromatography. In the dark, the hydroboration reaction gave a 62% yield, while irradiation decreased the yield to 44%.

Based on DFT calculations, the decreased reactivity of the closed form of the catalyst has been tentatively assigned to its electronic features, namely to the extended π -conjugation over the dithiophene backbone that decreases the electron density at the metal center.



	catalyst	conversion
1	C20 + $tBuOK$ + catecholborane	62%
2	C20 + $tBuOK$ + catecholborane $h\nu$, 365 nm, 20 min	44%

Scheme 31. Copper-catalyzed hydroboration of 4-fluorostyrene.

4.3. Catalysts based on biindane-diphosphines

4.3.1. Palladium-promoted Heck reactions

The biindane-derived macrocyclic diphosphine (*S*)-**20** displays an (*S*)-configured biaryl and a *cis* olefin moiety. When irradiated at $\lambda = 365$ nm in CH_2Cl_2 , it undergoes isomerization into a mixture of two *trans*-isomers with opposite configurations of the olefinic units. (Note that the stiff olefinic moiety adopts a non-planar, chiral configuration.) The photostationary state, reached after 40 min irradiation, contains a 68:23:9 mixture of *cis*-**20**, *trans*-**20**¹ and *trans*-**20**² (Scheme 32).^[26]

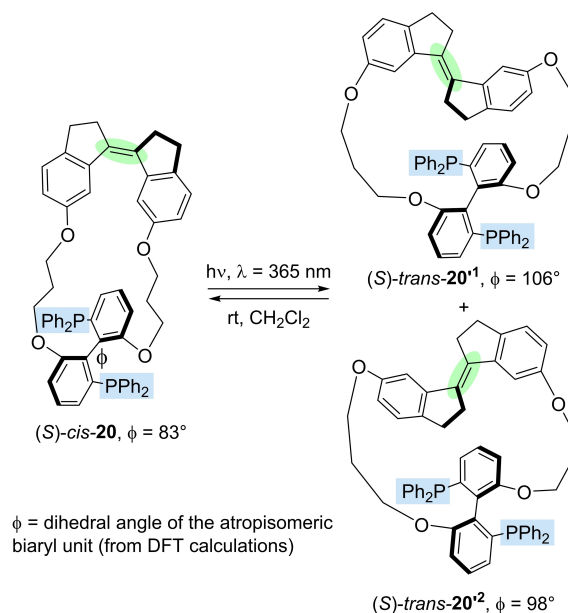
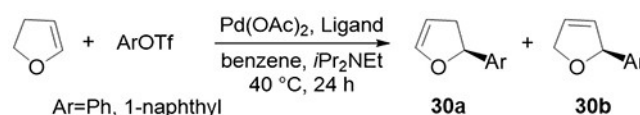
According to DFT calculations, the three diphosphines have significantly different dihedral angles at the biaryl moiety, with $\phi = 83^\circ$ for *cis*-**20** (compressed angle), $\phi = 106^\circ$ for *trans*-**20**¹ (extended) and $\phi = 98^\circ$ for *trans*-**20**² (virtually undistorted). These compounds have been separated and two of them have been tested as ligands in the enantioselective Pd-promoted Heck reactions in Scheme 33. Also, *in situ* switch experiments have been carried out to evaluate the catalytic activity of the mixture of palladium catalysts, presumably generated from *trans*-**20**¹ under irradiation.

From the Heck reactions in Scheme 33, the level of chiral induction has been correlated to the mechanical distortion of the dihedral angle of the biaryls, induced by photoisomerization. In the reaction between dihydrofuran and phenyl triflate (entries 1–4 in Scheme 33), the ligand with the more compressed dihedral angle, *cis*-**20**, afforded the 2,3-dihydrofuran **29a** with the highest enantiomeric excess (96% ee), while *trans*-**20**¹ afforded **29a** with only 79% ee. Moreover, it has been shown that *in situ* irradiation of the catalyst formed from *trans*-**20**¹ increases the enantioselectivity level, giving an intermediate 90% ee. The observed effect is assigned exclusively to geometrical changes of the dihedral angles, since the electronic properties of the two isomeric ligands are identical (identical $J_{p-se} = 739$ Hz for the corresponding selenides).

Analogous trends have been observed in the Heck reactions involving 1-naphthyl triflate (entries 5–8 in Scheme 33). In this case, the dihedral angles of the ligands affect also the **30a**:**30b** product ratios. Ligands with larger dihedral angles (*trans*-**18'**) favor indeed the 2,3-dihydrofuran **30a** vs 2,5-dihydrofuran **30b**.

In parallel studies, the same ligands *cis*-**20** and *trans*-**20**¹ have been compared in model allylic alkylation. However, in these reactions the mechanical distortion of the ligands induced only modest changes of the enantioselectivity levels.

This work demonstrates that externally induced photo-switch of a remote structural unit of the ligand can result in the effective actuation of a chiral metal catalyst.

Scheme 32. Photoisomerization of the biindane-derived diphosphine **20**.

	Ligand	Dihedral angle ϕ	Conv %	30a : 30b ratio	Ee % (<i>S</i> - 30a)
				Ar=Ph	
1	MeOBiphep	97°	23	95:5	90
2	<i>cis</i> - 20	83°	55	97:3	96
3	<i>trans</i> - 20 ¹	106°	95	98:2	79
4	<i>trans</i> - 20 ¹ + $h\nu$ ^[a]	-	93	97:3	90
				Ar=1-naphthyl	
5	MeOBiphep		98	79:21	54
6	<i>cis</i> - 20		91	72:28	60
7	<i>trans</i> - 20 ¹		>99	88:12	13
8	<i>trans</i> - 20 ¹ + $h\nu$ ^[a]		>99	85:15	42

[a] irradiation at 365 nm, 3W, 60s

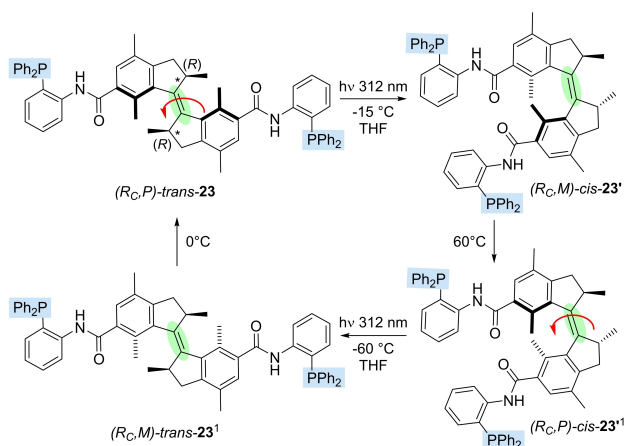
Scheme 33. Effect of the dihedral angle of the ligands on the enantioselectivity of Heck reactions.

4.3.2. Palladium-promoted desymmetrization of allylic carbamates

The second example hereafter also relates to enantioselectivity switch using chiral biindane-derived ligands.

The biindane-based diphosphine **23**^[27] behaves as a light-driven molecular motor, switching reversibly between four different forms, under combined photochemical and thermal conditions (Scheme 34). It displays both a stereogenic carbon with (*R*)-configuration and a hindered olefinic unit with helical chirality (*P* or *M*-configurations).

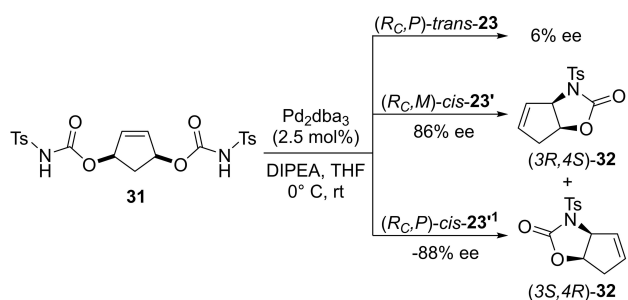
Under UV irradiation (312 nm), the starting diphosphine (*R_CP*)-*trans*-**23** undergoes photoisomerization into its *cis*-isomer (*R_CM*)-*cis*-**23'** (7:93 *trans*:*cis* ratio at the PSS). The



Scheme 34. Four-step cycle of rotary motion of diphosphine 23.

process involves a counterclockwise rotation of the indane fragment around the olefin C=C axis and leads therefore to inversion of the helical configuration (demonstrated by circular dichroism spectra). The rotation sense is dictated by the (*R*)-configured stereogenic carbon. Then, the (*R_C,M*)-*cis*-23' isomer tends to convert into the other *cis* isomer (*R_C,P*)-*cis*-23'¹ by thermal inversion of its helical configuration. From this compound, a second photochemical step generates the diphosphine (*R_C,M*)-*trans*-23'¹ that couldn't be isolated because it converts into the starting (*R_C,P*)-*trans*-23 below room temperature. The whole process has been monitored by NMR, UV and CD spectroscopy.

The isolated diphosphines (*R_C,P*)-*trans*-23, (*R_C,M*)-*cis*-23' and (*R_C,P*)-*cis*-23'¹ have been tested separately in the enantioselective intramolecular allylic amination of the *meso*-carbamate 31 (Scheme 35), with palladium catalysts generated *in situ* from Pd₂dba₃ and the ligands. As expected, the less hindered *trans* diphosphine (*R_C,P*)-*trans*-23 gives a nearly racemic oxazolidinone (6% ee), while the (*R_C,M*)-*cis*-isomer 23', formed by photoisomerization, promotes the reaction with excellent stereocontrol: (*3R,4S*)-32 was obtained in 90% yield and 86% ee. Finally, the (*R_C,P*)-*cis*-isomer 23'¹, thermally generated from (*R_C,M*)-*cis*-23', also gives excellent ee and opposite stereochemical control: (*3S,4R*)-32 was obtained in

Scheme 35. Stereodivergent synthesis of oxazolidinones via palladium promoted desymmetrization of the *meso* bis-carbamate 31.

85% yield and 88% ee. This result indicates that the sense of chiral induction is dictated mainly by the helical configuration of the biindane unit.

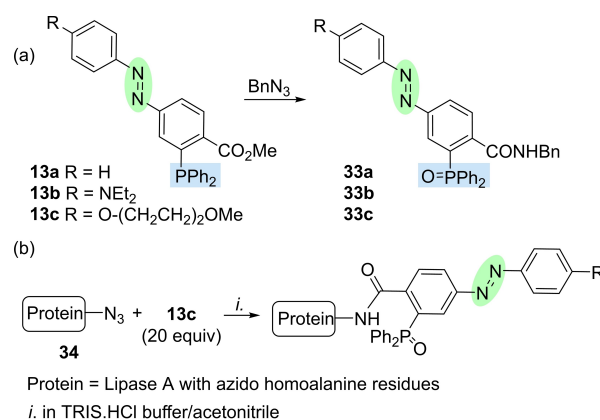
In summary, these studies have highlighted a photoresponsive chiral biindane diphosphine, 23, that achieves unidirectional rotation around its double bond under UV irradiation. The photoswitch provides an isomeric ligand giving largely improved enantioselectivity levels. This process couldn't be translated into an effective catalytic *in situ* photoswitch procedure, because the palladium catalyst showed only moderate stability under UV and heating.

5. Non-catalytic applications in organic synthesis

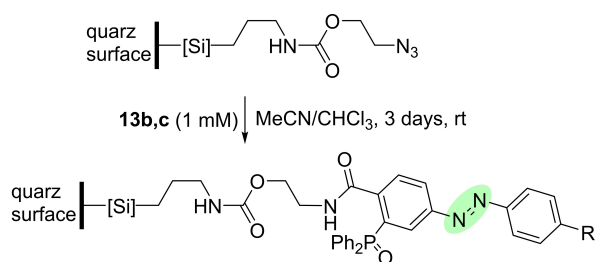
Beside their use as ligands in organometallic catalysis, azobenzene derived phosphines have found relevant synthetic applications as Staudinger-type reagents. Thus, B.L. Feringa envisioned the Staudinger-Bertozzi ligation as a tool to incorporate photoswitchable azobenzene tags in biological systems.^[39] The method consists in reacting the ester-functionalized azobenzene-phosphines 13 with biomolecules displaying azido functions (Scheme 36b).

Azido homoalanine residues (AHA) were introduced at positions 1, 9 and/or 79 of Lipase A from *Bacillus subtilis*. The azido-modified proteins 34 were incubated then with phosphine 13c in a TRIS.HCl buffer /acetonitrile mixture (pH 7.5, TRIS = *tris*(hydroxymethyl)aminomethane) for 22 h. This procedure led to incorporation of up to three azobenzene molecular switches into the enzyme. Singly, doubly and triply modified bioconjugated could be identified by ESI/MS deconvolution.

The photoswitch process has not been investigated so far on these azobenzene-modified proteins. However, it has been demonstrated that the model azobenzene amide 33a (Scheme 36a) displays efficient photoswitch under irradiation at $\lambda = 365$ nm (80% *cis*-isomer at the PSS state in aqueous



Scheme 36. Azobenzene-derived phosphines for the Staudinger-Bertozzi ligation: (a) model reaction; (b) reactions on azido-functionalized proteins.



Scheme 37. Modification of quartz surfaces with azobenzenes, via the Staudinger-Bertozzi ligation.

buffer). The thermal Z→E conversion is slow, but it can be accelerated by irradiation with white light. These features are highly suitable for the targeted biochemical applications. Further studies^[22] highlighted then that the switch process, and the stability of the Z-forms of the phosphine oxides **33** depend crucially on the nature of the R substituent. Interestingly, the amino-substituted azobenzene **33b** could be isomerized under visible light (532 nm).

The same phosphines **13** have been used to introduce azobenzene photoswitches into an homoalanine-modified peptide (Sp1-f3 zinc finger), as well as on suitably functionalized quartz surfaces, as illustrated in Scheme 37.^[22,39] Surface changes resulting from E- to Z-isomerization have been highlighted under irradiation at 365 nm.

In summary, azobenzene-derived phosphines allow the introduction of azobenzene units in biologically relevant substrates through Staudinger-Bertozzi ligations. Nevertheless, biomedical applications of these azobenzene tags still face highly challenging requirements, such as the thermal stability of Z-azobenzenes in aqueous biological media and implementation of photoresponsive processes under the deeper penetrating visible light.

Phosphorus functionalized azobenzenes have been considered also for applications in material sciences that are outside the scope of this minireview.

6. Conclusions

The remote spatio-temporal control of catalytic reactions by means of photoresponsive catalysts represents today a major but still challenging objective. As demonstrated by this short survey, photoswitchable phosphines might play a significant role in the field, as privileged ligands for transition metal complexes enabling highly diverse catalytic processes. Thus, for instance, photoinduced isomerization of phosphine-coordinated catalysts has allowed to regulate the rates of the Rh-promoted hydrogenation of CO₂ (section 4.1.2), Ru-promoted release of H₂ from ammonia-borane (section 4.1.3), Pd-promoted decarboxylations (section 4.1.1) and copper promoted hydroborations of styrenes (section 4.2.1) The *in situ* E→Z isomerization of azobenzene-diphosphine gold complexes has been shown to accelerate an intramolecular hydroamination reaction (section 4.1.4). Moreover, photo-

isomerization of biindane-derived ligands has been shown to control product ratios and enantioselectivity levels in Heck reactions, as well as in some intramolecular allylic aminations, under Pd-catalysis (sections 4.3.1 and 4.3.2).

When the phosphorus functions are close to the photo-switch units, photoisomerization is expected to induce significant changes of both geometrical features and electronic properties of the ligands. A clear-cut example is that of dithienylcyclopentene derived phosphines, where the closed forms display lower σ-donating ability than the open forms. Nevertheless, this well-established effect must not conceal that, in most instances, the observed changes of the catalytic behavior have not been correlated explicitly to tuning of the stereoelectronic descriptors^[40] of the ligands. Most often, only rather speculative rational has been given, and therefore the rational design of switchable ligands remains largely unattainable.

To find rational to catalytic behaviors is even more challenging when the photoswitch unit is remote from the phosphorus functions and the catalytic activity is modulated by subtle conformational changes of the ligand backbones in the outer coordination sphere (sections 4.1.2, 4.3.1 and 4.3.2).

Another current limitation of *in situ* photoswitch catalysis is that irradiation usually leads to incomplete isomerization of the catalysts (mixtures are formed at the photostationary states), which lowers consequently the amplitude of the photochemically-induced catalytic tuning. Also, thermal back-isomerization can take place spontaneously, notably with azobenzene-derived ligands, if continuous irradiation can't be applied during the whole catalytic process.

As a consequence of these practical limitations, but also of an insufficient differentiation of the isomeric forms of the ligands, a pure 'on-off' catalytic system based on photo-switchable phosphines remains to be demonstrated. Toward this goal, the design of new and improved ligands is eagerly awaited.

Although sparse, the pioneering reports summarized in this minireview highlight the huge potential of photo-responsive phosphorus ligands, the scope and current limitations of the field, and pave the way to further investigations.

Acknowledgements

Authors acknowledge financial support from ANR (Switch-Phos ANR-17-CE07-0032) and CHARMMMAT Labex (ANR-11-LABX-0039).

Conflict of Interest

The authors declare no conflict of interest.

Keywords: photoswitchable phosphines · azobenzenes · dithienylethenes · biindanes · organometallic catalysis

- [1] a) W. Szymański, J. M. Beierle, H. A. V. Kistemaker, W. A. Velema, B. L. Feringa, *Chem. Rev.* **2013**, *113*, 6114–6178; b) K. Hüll, J. Morstein, D. Trauner, *Chem. Rev.* **2018**, *118*, 10710–10747.
- [2] X. Huang, T. Li, *J. Mater. Chem. C* **2020**, *8*, 821–848.
- [3] a) D. Dattler, G. Fuks, J. Heiser, E. Moulin, A. Perrot, X. Yao, N. Giuseppone, *Chem. Rev.* **2020**, *120*, 310–433; b) S. Erbas-Cakmak, D. A. Leigh, C. T. McTernan, A. L. Nussbaumer, *Chem. Rev.* **2015**, *115*, 10081–10206; c) F. Lancia, A. Ryabchun, N. Katsonis, *Nature Rev. Chem.* **2019**, *3*, 536–551; d) M. S. Baroncini, S. A. Credi, *Chem. Rev.* **2020**, *120*, 200–268.
- [4] H. Nie, J. L. Self, A. S. Kuenstler, R. C. Hayward, J. R. de Alaniz, *Adv. Opt. Mater.* **2019**, *7*, 1900224.
- [5] C.-L. Sun, C. Wang, R. Boulatov, *ChemPhotoChem* **2019**, *3*, 268–283.
- [6] a) R. S. Stoll, S. Hecht, *Angew. Chem. Int. Ed.* **2010**, *49*, 5054–5075; *Angew. Chem.* **2010**, *122*, 5176–5200; b) B. M. Neilson, C. W. Bielawski, *ACS Catal.* **2013**, *3*, 1874–1885; c) V. Blanco, D. A. Leigh, V. Marcos, *Chem. Soc. Rev.* **2015**, *44*, 5341–5370; d) R. Dorel, B. L. Feringa, *Chem. Commun.* **2019**, *55*, 6477–6486; e) Z. Freixa, *Catal. Sci. Technol.* **2020**, *10*, 3122–3139.
- [7] D. Sud, T. B. Norsten, N. R. Branda, *Angew. Chem. Int. Ed.* **2005**, *44*, 2019–2021; *Angew. Chem.* **2005**, *117*, 2055–2057.
- [8] a) B. M. Neilson, C. W. Bielawski, *J. Am. Chem. Soc.* **2012**, *134*, 12693–12699; b) B. M. Neilson, C. W. Bielawski, *Organometallics* **2013**, *32*, 3121–3128; c) A. J. Teator, H. Shao, G. Lu, P. Liu, C. W. Bielawski, *Organometallics* **2017**, *36*, 490–497.
- [9] a) R. S. Stoll, M. V. Peters, A. Kuhn, S. Heiles, R. Goddard, M. Bühl, C. M. Thiele, S. Hecht, *J. Am. Chem. Soc.* **2009**, *131*, 357–367; b) J. Wang, B. L. Feringa, *Science* **2011**, *331*, 1429–1432; c) T. Imahori, R. Yamaguchi, S. Kurihara, *Chem. Eur. J.* **2012**, *18*, 10802–10807; d) D. Wilson, N. R. Branda, *Angew. Chem. Int. Ed.* **2012**, *51*, 5431–5434; *Angew. Chem.* **2012**, *124*, 5527–5530; e) L. Osorio-Planes, C. Rodríguez-Escrich, M. A. Pericàs, *Org. Lett.* **2014**, *16*, 1704–1707; f) R. Dorel, B. L. Feringa, *Angew. Chem. Int. Ed.* **2020**, *59*, 785–789; g) M. Vlatkovic, J. Volarić, B. S. L. Collins, L. Bernardi, B. L. Feringa, *Org. Biomol. Chem.* **2017**, *15*, 8285–8294.
- [10] H. M. D. Bandara, S. C. Burdette, *Chem. Soc. Rev.* **2012**, *41*, 1809–1825.
- [11] a) M. Irie, *Chem. Rev.* **2000**, *100*, 1685–1716; b) H. Tian, S. Yang, *Chem. Soc. Rev.* **2004**, *33*, 85–97; c) M. Irie, T. Fukaminato, K. Matsuda, S. Kobatake, *Chem. Rev.* **2014**, *114*, 12174–12277.
- [12] a) C. García-Iriepa, M. Marazzi, L. M. Frutos, D. Sampedro, *RSC Adv.* **2013**, *3*, 6241–6266; b) V. García-López, D. Liu, J. M. Tour, *Chem. Rev.* **2020**, *120*, 79–124; c) D. Villarón, S. J. Wezenberg, *Angew. Chem. Int. Ed.* **2020**, *59*, 13192–13202.
- [13] a) M. J. Alder, K. R. Flower, R. G. Pritchard, *Tetrahedron Lett.* **1998**, *39*, 3571–3574; b) M. J. Alder, W. I. Cross, K. R. Flower, R. G. Pritchard, *J. Chem. Soc. Dalton Trans.* **1999**, 2563–2573; c) M. J. Alder, V. M. Bates, W. I. Cross, K. R. Flower, R. G. Pritchard, *J. Chem. Soc. Perkin Trans. 1* **2001**, 2669–2675.
- [14] M. Kawamura, R. Kiyotake, K. Kudo, *Chirality* **2002**, *14*, 724–726.
- [15] a) K. Chane-Ching, M. Lequan, R. M. Lequan, C. Runser, M. Barzoukas, A. Fort, *J. Mater. Chem.* **1995**, *5*, 649–652; b) M. Lequan, R. M. Lequan, K. Chane-Ching, P. Bassoul, G. Bravic, Y. Barrans, D. Chasseau, *J. Mater. Chem.* **1996**, *6*, 5–9; c) C. Lambert, E. Schmäzlin, K. Meerholz, C. Bräuchle, *Chem. Eur. J.* **1998**, *4*, 512–521.
- [16] M. Yamamura, N. Kano, T. Kawashima, *Inorg. Chem.* **2006**, *45*, 6497–6507.
- [17] T. Arif, C. Cazorla, N. Bogliotti, N. Saleh, F. Blanchard, V. Gandon, R. Métivier, J. Xie, A. Voituriez, A. Marinetti, *Catal. Sci. Technol.* **2018**, *8*, 710–715.
- [18] a) M. D. Segarra-Maset, P. W. N. M. van Leeuwen, Z. Freixa, *Eur. J. Inorg. Chem.* **2010**, 2075–2078; b) A. Telleria, P. W. N. M. Van Leeuwen, Z. Freixa, *Dalton Trans.* **2017**, *46*, 3569–3578.
- [19] a) M. Yamamura, N. Kano, T. Kawashima, *J. Am. Chem. Soc.* **2005**, *127*, 11954–11955; b) M. Yamamura, N. Kano, T. Kawashima, *Bull. Chem. Soc. Jpn.* **2012**, *85*, 110–123.
- [20] E. Besson, A. Mehdi, V. Matura, Y. Guari, C. Reyé, R. J. P. Corriu, *Chem. Commun.* **2005**, 1775–1777.
- [21] H. Bricout, E. Banaszak, C. Len, F. Hapiot, E. Monflier, *Chem. Commun.* **2010**, *46*, 7813–7815.
- [22] C. Poloni, W. Szymański, L. Hou, W. R. Browne, B. L. Feringa, *Chem. Eur. J.* **2014**, *20*, 946–951.
- [23] D. Sud, R. McDonald, N. R. Branda, *Inorg. Chem.* **2005**, *44*, 5960–5962.
- [24] J. Yin, Y. Lin, X. Cao, G.-A. Yu, H. Tu, S. H. Liu, *Dyes Pigm.* **2009**, *81*, 152–155.
- [25] G. Bianchini, G. Strukul, D. F. Wass, A. Scarso, *RSC Adv.* **2015**, *5*, 10795–10798.
- [26] Z. S. Kean, S. Akbulatov, Y. Tian, R. A. Widenhoefer, R. Boulatov, S. L. Craig, *Angew. Chem. Int. Ed.* **2014**, *53*, 14508–145011; *Angew. Chem.* **2014**, *126*, 14736–14739.
- [27] D. Zhao, T. M. Neubauer, B. L. Feringa, *Nat. Commun.* **2015**, *6*, 6652 doi: 6610.1038/ncomms7652.
- [28] M. Vlatkovic, L. Bernardi, E. Otten, B. L. Feringa, *Chem. Commun.* **2014**, *50*, 7773–7775.
- [29] R. Costil, S. Crespi, L. Pfeifer, B. L. Feringa, *Chem. Eur. J.* **2020**, *26*, 7783–7787.
- [30] M. J. Alder, W. I. Cross, K. R. Flower, R. G. Pritchard, *J. Organomet. Chem.* **1999**, *590*, 123–128.
- [31] M. J. Alder, K. R. Flower, R. G. Pritchard, *J. Organomet. Chem.* **2001**, *629*, 153–159.
- [32] M. J. Alder, W. I. Cross, K. R. Flower, R. G. Pritchard, *J. Organomet. Chem.* **1998**, *568*, 279–285.
- [33] N. Kano, M. Yamamura, X. Meng, T. Yasuzuka, T. Kawashima, *Dalton Trans.* **2012**, *41*, 11491–11496.
- [34] J. Liang, J. Yin, Z. Li, C. Zhang, D. Wu, S. H. Liu, *Dyes Pigm.* **2011**, *91*, 364–369.
- [35] F.-R. Dai, B. Li, L.-X. Shi, L.-Y. Zhang, Z.-N. Chen, *Dalton Trans.* **2009**, 10244–10249.
- [36] B. Li, Y.-H. Wu, H.-M. Wen, L.-X. Shi, Z.-N. Chen, *Inorg. Chem.* **2012**, *51*, 1933–1942.
- [37] N. Priyadarshani, B. Ginovska, J. T. Bays, J. C. Linehan, W. J. Shaw, *Dalton Trans.* **2015**, *44*, 14854–14864.
- [38] Z. Xu, Y. Cao, B. O. Patrick, M. O. Wolf, *Chem. Eur. J.* **2018**, *24*, 10315–10319.
- [39] W. Szymański, B. Wu, C. Poloni, D. B. Janssen, B. L. Feringa, *Angew. Chem. Int. Ed.* **2013**, *52*, 2068–2072; *Angew. Chem.* **2013**, *125*, 2122–2126.
- [40] a) D. J. Durand, N. Fey, *Chem. Rev.* **2019**, *119*, 6561–6594; b) L. Falivene, Z. Cao, A. Petta, L. Serra, A. Poater, R. Oliva, V. Scarano, L. Cavallo, *Nat. Chem.* **2019**, *11*, 872–879.

Manuscript received: April 9, 2020
Revised manuscript received: August 19, 2020
Version of record online: September 25, 2020